JOC Article

Regioselectivity in the Ligand-Assisted Addition of Vinylmagnesium Bromide: An Experimental and Theoretical Study on the γ-Alkoxycyclobutenone Model

Teresa Varea,[†] Ana Alcalde,[†] Amparo Grancha,[†] Julio Lloret,[†] Gregorio Asensio,*[,†] and Agusti Lledos*[,‡]

Departamento de Química Orgánica, Universidad de Valencia, Avda. V.A. Estellés s/n 46100-Burjassot, Spain, and Departament de Química, Edifici Cn, Universitat Autónoma de Barcelona, 08193 Bellaterra, Spain

gregorio.asensio@uv.es; agusti@klingon.uab.es

Received March 18, 2008

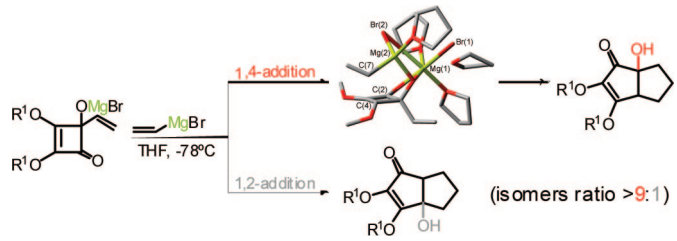

Compounds **2** (M = Mg) obtained in the mono addition of vinylmagnesium bromide to squarates are attractive structural models to determine the influence of complexation between magnesium(II) and the alkoxide group on the regioselectivity of the 1,2- versus 1,4-addition of organomagnesium by complex induced proximity effects (CIPE). The 1,4-addition is observed almost exclusively in the case of vinylmagnesium in THF solution with formation of hydroxyketones type **5**, which are always side or minor products in the known reaction of alkenyllithium derivatives. A comparative study on the reactivity of alkenyllithium and magnesiun derivatives is reported. The high regioselectivitity observed in the 1,4-addition of vinylmagnesium bromide is fully understood by computational studies of compounds **2** (M = Mg) at the DFT level with the density functional B3LYP.

Introduction

The conjugate addition of carbon nucleophiles to α,β-unsaturated carbonyl compounds is a general C−C bond-formation method. The ambident nature of these carbonyl compounds is perhaps the main drawback of the procedure since it introduces the problem of controlling the regioselectivity.[1] Organolithium derivatives tend to give 1,2-addition products that can be reversed by using different tricks and techniques.[2] However, the regiochemistry of reactions carried with Grignard reagents as a source of nucleophilic carbon is difficult to predict.[3] In many cases, the addition of copper salts usually leads to a 1,4-addition of organomagnesium derivatives with high regioselectivity and excellent yields.[4] Another strategy is to introduce a substituent next to the reactive position in the substrate to control the regioselectivity by magnesium complexation. For instance, Liotta et al.[5] showed that it is possible to control the position and the face of the attack of organomagnesium compounds to enones derived from *p*-quinones **A** by ligand-assisted nucleophilic addition (LANA) due to the alkoxyl group. Excellent results have been reported more recently by Fleming et al.[6] in the conjugate addition of organomagnesium compounds to γ-hydroxy-substituted unsatur-

[†] Universidad de Valencia.
[‡] Universitat Autónoma de Barcelona.

(1) (a) Lee, V. J. Conjugate Additions of Reactive Carbanions to Activated Alkenes and Alkynes. In *Comprehensive Organic Synthesis*; Trost, B. M., Fleming, I. Eds.; Pergamon Press: New York, 1991; Vol. 1, Chapter 1.2, p 69. (b) Chatfield, D. C.; Augsten, A.; D′Cunha, C.; Lewandowska, E.; Wnuk, S. F. *Eur. J. Org. Chem.* **2004**, 313.

(2) Tomioka, K.; Shioya, Y.; Nagaoka, Y.; Yamada, K. *J. Org. Chem.* **2001**, *66*, 7051, and references therein.

(3) Negishi, E.-I. In *Organometallics in Organic Synthesis*; John Wiley: New York, 1980; Vol. I, p 127.

(4) Perlmutter, P. In *Conjugate Addition Reactions in Organic Synthesis*; Pergamon Press: New York, 1992; Tetrahedron Organic Chemistry Series, Vol. 9, p 35.

(5) (a) Solomon, M.; Jamison, W. C. L.; McCormick, M.; Liotta, D.; Cherry, D. A.; Mills, J. E.; Shah, R. D.; Rodgers, J. D.; Maryanoff, C. A. *J. Am. Chem. Soc.* **1988**, *110*, 3702. (b) Swiss, K. A.; Liotta, D. C.; Maryanoff, C. A. *J. Am. Chem. Soc.* **1990**, *112*, 9393.

10.1021/jo800617y CCC: $40.75 © 2008 American Chemical Society
Published on Web 07/29/2008

ated nitriles. Regioselectivity is attributed to the formation of an intermediate alkyl magnesium alkoxide **B** from which the alkyl group is delivered. These reactions can be considered in a general group in which regioselectivity is controlled by the so-called complex induced proximity effects (CIPE).[7]

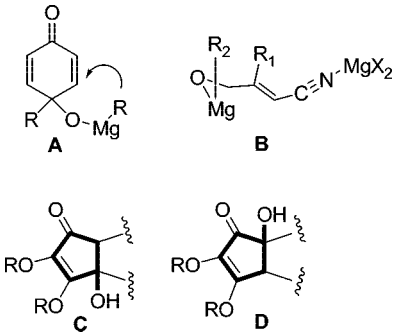

Many uses of squaric acid esters **1** have been reported in organic synthesis. The double addition of alkenyllithium derivatives to squarates[8] has been extensively investigated by Paquette et al.,[9,10] who by this methodology described the synthesis of a great variety of bicyclic and polycyclic compounds containing the hydroxycyclopentenone moiety **C** or **D**. The position of the angular hydroxyl group, according to the accepted reaction mechanism,[9] depends on the regiochemistry of the addition of the second equivalent of alkenyllithium to the intermediate α,β-unsaturated alkoxide **2**. The 1,2-addition of alkenyllithium to **2** leads to the formation of the regioisomers **C**, while the 1,4-addition yields the regiosiomers **D**. The 1,2-addition to the C=O group is the main reaction path for simple alkenyllithium derivatives, which consequently leads to type **C** compounds and to only minor amounts of the regioisomers **D**.[10b]

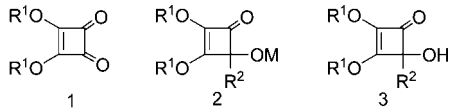

As a result of the excellent yields and regioselectivity attained in these processes, Paquette's methodology becomes a method of choice in the preparation of bicyclic compounds containing the hydroxycyclopentenone moiety **C**. To date, the use of magnesium compounds in the addition to squarates has proved less successful. Selectivity depends on the size of the alkyl group in the squarate ester.[11,12] Monoaddition compounds **2** (M = Mg) are attractive structural models to determine the influence of complexation between magnesium(II) and the alkoxide group on the regioselectivity of the 1,2- versus 1,4-addition of a second organomagnesium equivalent by CIPE. In this context we believed that studying the course of the addition of a second equivalent of vinylmagnesium derivatives to 1,2-adducts **2** (M = Mg) by experimental and computational methods was of interest for a better understanding of the factors controlling the selectivity.

CHART 1. Possible Intramolecular Coordination Models for Magnesium Alkoxides 2

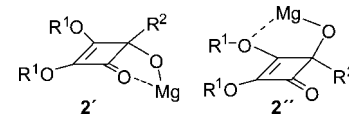

Results and Discussion

Addition of 2 equiv of Vinylmagnesium Derivatives to Squarates 1. The behavior of the 1,2-adducts **2** in the addition of the second equivalent of organomagnesium compounds is intriguing since they are α,β-unsaturated carbonyl compounds substituted by one alkoxyl group that may, at first, be able to direct the addition to either the carbonyl or olefinic carbon. For geometrical reasons, one should not expect any remarkable regioselectivity when using a simplified model since (i) the alkoxide oxygen atom, coordinated with magnesium, is placed at a similar distance to both electrophilic centers in the cyclobutenone moiety, and (ii) at least two different types of coordination with magnesium(II) can be depicted as shown in structures **2′** and **2″** in which the O−Mg distances are 2.1 and 2.3 Å, respectively (Chart 1).

The stability of these two complexes will differ as we consider the orientation of the p-orbitals containing the lone electron pairs of the coordinating oxygen atoms as well as their different basicity related to the mono- or dicoordinated character of the heteroatom in **2′** and **2″**.

The results obtained from adding 2 equiv of vinyllithium or vinylmagnesium bromide in diethyl ether or THF solution to squaric acid esters **1a**−**c** are reported in Table 1. GC and NMR analyses of the crude reaction mixtures showed the formation of bicyclic octenones **5** and **7** in a variable ratio (see Scheme 1). Only the 1,2-addition of the first equivalent of organometallic (M = Li or Mg) occurs in all cases. Conversely, reverse regioselectivity was observed for the addition of the second equivalent of the lithium or magnesium reagent.

With alkenyllithium, bicyclic γ-hydroxyketones **7**[9,10] are obtained with an excellent regioselectivity within a >99:1 to 89:11 ratio. By contrast, when we carried out the addition of 2 equiv of vinylmagnesium to squarates in THF at low temperature (−78 °C) (see Scheme 1, eq 1), hydroxyketones **5** were obtained by 1,2-/1,4-addition also with an excellent regioselectivity.

The size of the alkyl substituent in the starting squarates does not influence the selectivity of the double addition of vinyl-

(6) (a) Fleming, F. F.; Wang, Q.; Zhang, Z.; Steward, O. W. *J. Org. Chem.* **2002**, *67*, 5953. (b) Fleming, F. F.; Gudipati, V.; Steward, O. W. *Org. Lett.* **2002**, *4*, 659.

(7) Beak, P.; Meyers, A. I. *Acc. Chem. Res.* **1986**, *19*, 356.

(8) Varea, T.; Grancha, A.; Asensio, G. *Tetrahedron* **1995**, *51*, 12373.

(9) Paquette, L. A. *Eur. J. Org. Chem.* **1998**, 1709, and references therein.

(10) (a) Paquette, L. A.; Liu, Z.; Ramsey, C.; Gallucci, J. C. *J. Org. Chem.* **2005**, *70*, 8154. (b) Morwick, T. M.; Paquette, L. A. In *Organic Synthesis*; Shinkai, I., Ed.; Wiley-VCH: Weinheim, 1997; Vol. 74, p 169. (c) Paquette, L. A.; Morwick, T. M. *J. Am. Chem. Soc.* **1997**, *119*, 1230.

(11) Dehmolv, E. V.; Shell, H. G. *Chem. Ber.* **1980**, *113*, 1.

(12) Conflicting reports have appeared in the literature regarding the regiochemistry of the addition of organomagnesium compounds to squarates. Kraus reported the formation of the 1,4-monoaddition diketone (R^1 = Me, R^2 = Ph) in the reaction of phenyl magnesium bromide with squarate **1c** after a workup under acid conditions. Kraus, J. L. *Tetrahedron Lett.* **1985**, *26*, 1867. It is known that the hydrolysis of the 1,2-adducts in an acid medium gives rise to their transformation into asymmetric diketones leading to the misleading conclusion that a 1,4-addition took place:

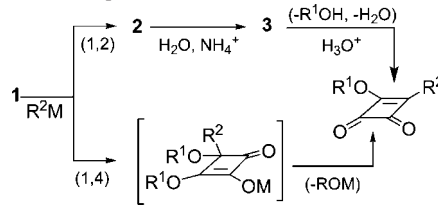

SCHEME 1. Double Addition of the Vinyl Reagent; Formation of Bicycloctenones 5 and 7

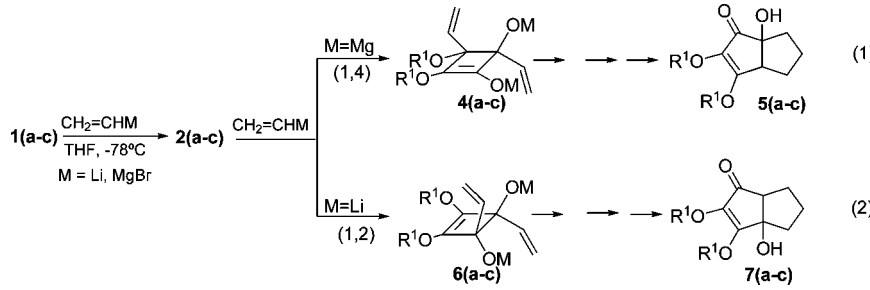

SCHEME 2. Attempted Reaction of Alcohols 8a and 9a with Vinylmagnesium Bromide

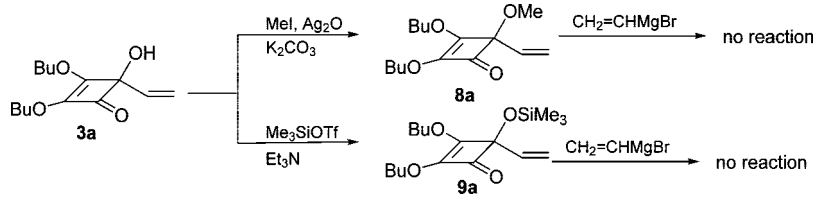

TABLE 1. Reactions of Dialkyl Squarates 1a−c with the Vinyl Metallic Reagent (CH_2=CHM)

entry	squarate	M	temp (°C)	solvent	yield (%)[a]	regioselectivity (**5**:**7**)[b]
1	**1a**	Li	−78	THF	61	6:94
2	**1b**	Li	−78	THF	49	5:95
3	**1c**	Li	−78	THF	45	1:>99
4	**1a**	MgBr	−78	THF	61 (>83)[c]	93:7
5	**1b**	MgBr	−78	THF	35	76:24[d]
6	**1c**	MgBr	−78	THF	65	92:8
7	**1a**	Li	22	THF	51	11:89
8	**1a**	MgBr	22	THF	69	75:25
9	**1a**	Li	−78	Et_2O	54	16:84
10	**1a**	MgBr	−78	Et_2O	61	65:35

[a] Total yield based on isolated bicycles. [b] Based on NMR and/or GC. [c] Yield based on GC (in parentheses). [d] Reaction carried out in Ar atmosphere. Other values of the regioselectivity obtained in N_2 atmosphere go from 47:53 to 56:44, depending on the source of vinylmagnesium bromide used.

lithium (see entries 1−3 in Table 1). Conversely, a high degree of selectivity for the conjugate addition is attained with the Grignard reagent in the additions to the *n*-butyl (**1a**) and methyl (**1c**) esters (entries 4 and 6, Table 1), but selectivity decreases for the bulkier isopropyl ester **1b** (entry 5, Table 1). It is reasonable to argue that a branched substituent placed at the olefinic carbon in **2** should make the conjugate addition difficult, a situation that affects the reactions with magnesium but not with lithium.

The addition of vinyllithium and vinylmagnesium to squarates **1** also differs in the effect of the temperature on regioselectivity. Reactions with vinyllithium are almost unaffected by changes in temperature in the −78 to 22 °C range. By contrast, the selectivity of the second addition of vinylmagnesium decreases significantly when the temperature increases from −78 °C to room temperature (entries 4 and 8, Table 1). Changing diethyl ether for THF as a solvent also leads to a lower selectivity for both organometallic derivatives (see entries 1 and 9 or 4 and 10, Table 1). This is also an interesting observation, however, since in general the conjugate addition of organolithium derivatives is favored by THF due to its higher ability when compared with that of ether to dissociate lithium aggregates, a fact related with the formation of conjugate addition products.[13] Conversely, the influence of the solvent on the 1,2- versus 1,4-selectivity in the second vinylmagnesium bromide addition to squarate **1a** follows the usual trend (entries 4 and 10, Table 1).[14]

The behavior of vinyllithium and vinylmagnesium differs with the second addition in THF solution. In fact, while the 1,2-addition mode predominates also with the addition of the second equivalent of vinyllithium, the 1,4-addition is observed almost exclusively in the case of vinylmagnesium when the size of the -OR substituent is small (entries 4 and 6, Table 1). In order to determine the influence of the presence of the alkoxide group in **2** on regioselectivity, we decided to study the reaction of the Grignard reagent with O-protected derivatives of alcohols **3** (Scheme 2).

Alcohol **3a** (R^1 = Bu, R^2 = -CH=CH_2) was prepared[15a] by reacting **1a** with vinylmagnesium bromide and was submitted to methylation (MeI, K_2CO_3, Ag_2O)[15b] or silylation (Me_3SiOTf, Et_3N) to give **8a** and **9a**, respectively. When vinylmagnesium bromide was added to either the methyl ether **8a** or trimethylsilyl ether **9a** in THF at −78 °C, the starting substrates were recovered unchanged after the usual workup. Products resulting from the addition of the Grignard reagent were not detected in any case (see eqs 3 and 4 in Scheme 2).

All the above results strongly suggested that the alkoxide group in adducts **2a** and **2c** determines the course of the second addition of the Grignard reagent and prompted us to perform a theoretical study of this reaction as a model to study the relationship between magnesium complexation and regioselectivity.

Theoretical Study of the Conjugate Addition of Vinylmagnesium Bromide to Alkoxide 2. Choice of Model. Despite the widespread use of organomagnesium derivatives in organic synthesis for more than a century and the extended use of computational methods to investigate reaction mechanisms, only scarce examples can be found in the computational chemistry literature applied to the study of the course of reactions involving Grignard reagents[16] or even the structure of these organometallics.[17] This lack of information is probably due to the

(13) Sikorski, W. H.; Reich, H. J. *J. Am. Chem. Soc.* **2001**, *123*, 6527.
(14) Gocmen, M.; Soussan, G. *J. Organomet. Chem.* **1974**, *80*, 303.
(15) (a) Peña-Cabrera, E.; Liebeskind, L. A. *J. Org. Chem.* **2002**, *67*, 1689. (b) Liebeskind, L. S.; Bombrun, A. *J. Org. Chem.* **1994**, *59*, 1149.

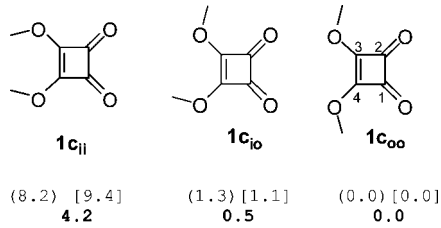

FIGURE 1. Conformational isomers of **1c** and their B3LYP/6-31G* gas-phase potential energies (ΔE) and Gibbs energies ($\Delta G_{(195)}$) relative to $\mathbf{1c_{oo}}$ (in kcal/mol) in parentheses and in brackets, respectively. The 6-31++G** energies in THF are in bold.

complexity of the behavior of magnesium derivatives owing to the Schlenk equilibrium and the existence of different aggregation states and coordination numbers, all these factors making it very difficult to identify the real reacting species in solution.[16a] Given this structural complexity, performing reliable DFT calculations with these reagents remains a challenging problem to date. Huang and Lu et al.[16b] have reported recently an interesting computational study of the mechanism of the regioselective asymmetric addition of Grignard reagents to maleimides. Magnesium coordination indexes 4−6 were used in this study. In this context we should mention the determination by Burk et al.[18a] of DFT solvation energies for MeMgBr, EtMgBr, and PhMgBr in THF solution, who concluded that magnesium was coordinated to two solvent molecules in the energetically most favorable situation. Moreover, Kato[18b] reported recently the application of the analytical RISM-MP2 free energy gradient method to the Schlenk equilibrium and tetrahedrally coordinated Mg atom in Grignard reagents was found to be the most stable species even in solution. The coordination index of 4 for magnesium is also found in most of the X-ray diffraction studies of organomagnesium compounds, especially when bulky ligands are present.[17b] On these grounds and to reduce computational costs, taking into account the complexity of the system subject of our study, models in which after the addition the coordination index of magnesium is at least 4 were used as a first approach. With this aim we chose $(CH_2CH)MgBr\cdot THF$ and $(CH_2CH)MgBr\cdot Et_2O$ as models of the real Grignard reagent in THF and Et_2O solvents, respectively. For the same reason, calculations were performed on methyl squarate (**1c**) as a model compound.

Thermodynamics and Kinetics of the First Addition. To study the addition of the first equivalent of vinylmagnesium bromide to methyl squarate, a conformational study of **1c** was first carried out. Three energy minima, $\mathbf{1c_{ii}}$, $\mathbf{1c_{io}}$, and $\mathbf{1c_{oo}}$ according to the *inward* or *outward* orientation of the methyl groups, were found, where $\mathbf{1c_{oo}}$ was the lowest energy conformation (see Figure 1). In this conformation the CH_3 groups of the methoxy substituents at C3 and C4 are oriented (*out*, *out*) toward the carbonyl groups.

TABLE 2. Selected Distances (Å) for Compounds in the 1,2- and 1,4-Pathways of the First Addition[a]

	$\mathbf{1c_{oo}\cdot Mg\text{-}A}$	$\mathbf{1c_{oo}\cdot Mg\text{-}B}$	1TS-1,2	1TS-1,4	Prod-1,2	Prod-1,4
d(Mg−C5)	2.119	2.109	2.217	2.349	3.681	5.080
d(Mg−O1)	2.069	2.117	1.989	2.058	1.952	2.014
d(Mg−O2	5.303	3.681	4.082	3.055	2.119	2.116
d(C1−O1)	1.228	1.232	1.273	1.281	1.364	1.305
d(C2−O2)	1.211	1.207	1.215	1.216	1.257	1.257
d(C1−C5)	4.259	4.364	2.312	3.055	1.514	3.323
d(C3−C5)	6.003	6.006	3.393	2.227	3.177	1.509

[a] Atom numbering is shown in Figure 4.

NPA charges and frontier orbitals HOMO and LUMO for the minimum energy conformation $\mathbf{1c_{oo}}$ are shown in Figure 2. Calculated NPA charges are +0.41 e and +0.25 e at the carbonyl (C1) and the conjugated carbon (C3), respectively. However, the coefficients in the LUMO are 0.31 and 0.50 for the contribution of p-orbitals of C1 and C3, respectively. The HOMO in **1c** results from the contributions of p-orbitals of the oxygen atoms and σ electrons of the cyclic framework. According to this description, the attack of the first equivalent of vinyllithium or vinylmagnesium to the carbonyl carbon seems to be controlled by the interaction between the metal, Li (I) or Mg(II), and the carbonyl moieties in the HOMO.[19]

Although only the 1,2-addition takes place with the addition of the first equivalent of vinylmagnesium, for comparative purposes we have theoretically studied the 1,2- and 1,4-pathways for the first addition. Investigation of the possible adducts resulting from the complexation of $(CH_2CH)MgBr\cdot THF$ to $\mathbf{1c_{oo}}$ has led to two intermediates($\mathbf{1c_{oo}\cdot Mg\text{-}A}$ and $\mathbf{1c_{oo}\cdot Mg\text{-}B}$, Figure 3 and Table 2). The first addition involves precomplexation of the magnesium to the carbonyl oxygen. In both complexes the magnesium atom is coordinated to only one carbonyl oxygen (distance Mg···O about 2.1 Å). Whereas in $\mathbf{1c_{oo}\cdot Mg\text{-}A}$ the organomagnesium is placed in the region between one carbonyl and one -OR substituent, in $\mathbf{1c_{oo}\cdot Mg\text{-}B}$ it is placed between the two carbonyls, although far way from the second carbonyl (3.7 Å) to discard bidentate coordination. $\mathbf{1c_{oo}\cdot Mg\text{-}A}$ is slightly more stable (3.2 kcal/mol) than $\mathbf{1c_{oo}\cdot Mg\text{-}B}$ both from 6 to 31G* gas-phase energies and Gibbs

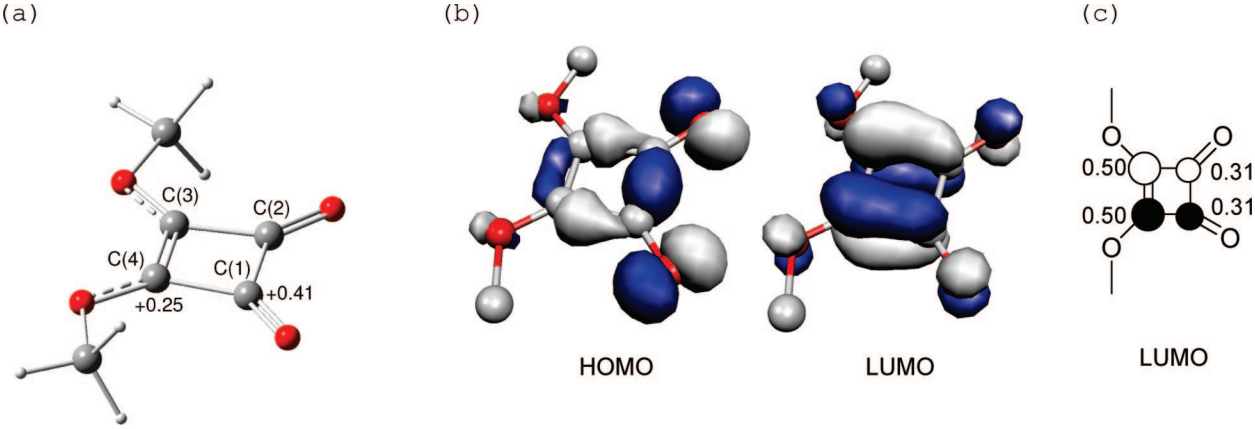

FIGURE 2. (a) B3LYP/6-31G*-optimized geometry of $\mathbf{1c_{oo}}$ showing NPA charges in C1 and C4. (b) HOMO and LUMO (isovalue 0.06) in the B3LYP/6-31G*-optimized geometry of $\mathbf{1c_{oo}}$. (c) Contribution to LUMO of the C1, C2, C3, and C4 atomic p-orbitals.

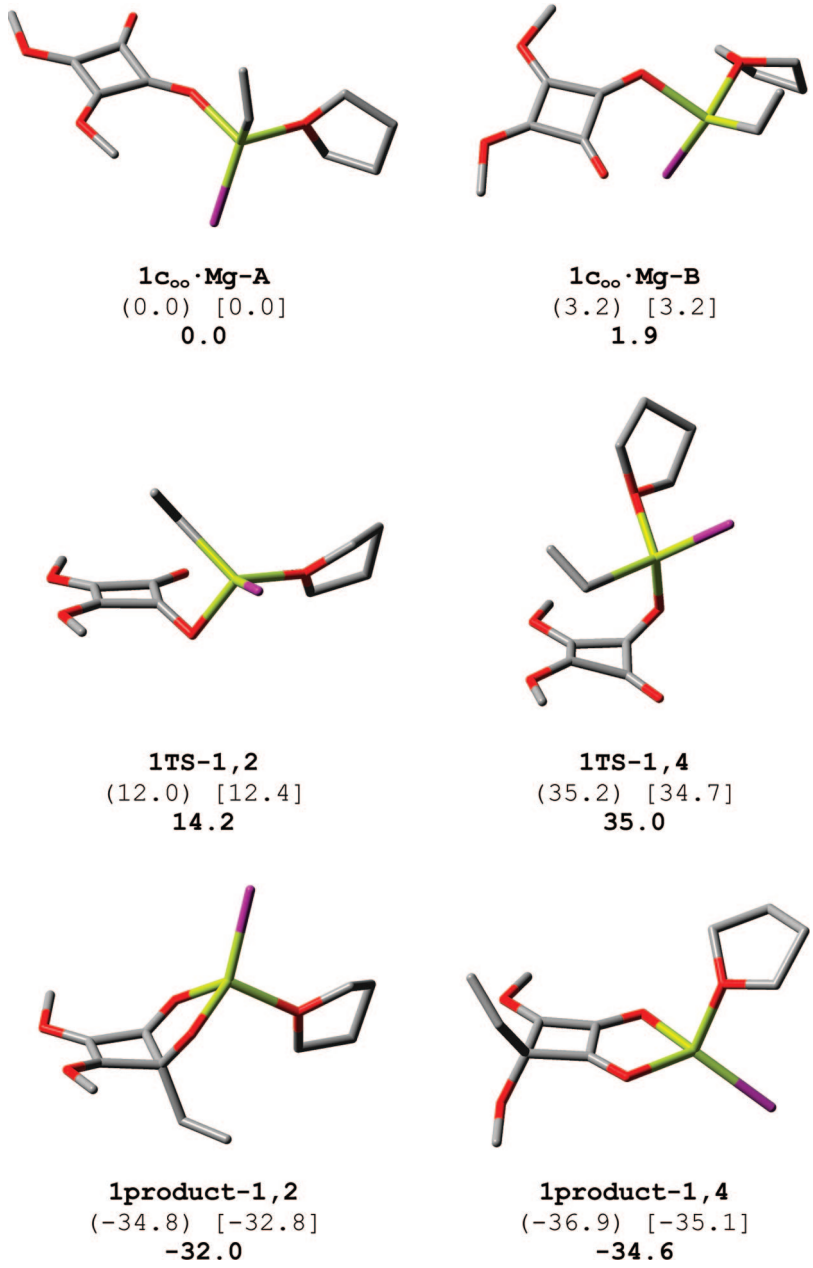

FIGURE 3. B3LYP/6-31G*-optimized geometries of intermediates (**1c$_{oo}$·Mg-A**, **1c$_{oo}$·Mg-B**), transition states (**1TS-1,2**; **1TS-1,4**) and products (**1product-1,2**, **1product-1,4**) for the first addition. The calculated gas-phase potential energies (ΔE) and Gibbs energies ($\Delta G_{(195)}$) relative to **1c$_{oo}$·Mg-A** (in kcal/mol) are given in parentheses and in brackets, respectively. The 6-31++G** energies in THF are in bold.

energies. In THF **1c$_{oo}$·Mg-A** is still 1.9 kcal/mol more stable than **1c$_{oo}$·Mg-B** (6-31++G** values). Both structures can interconvert easily with a small tilt of the Mg···C−O angle. Complexation of the vinylmagnesium derivative to the squarate is favored on both energy and Gibbs energy grounds. $\Delta G_{(195)}$ complexation of (CH_2CH)MgBr·THF to **1c$_{oo}$** to afford **1c$_{oo}$·Mg-A** is −6.0 kcal/mol (gas-phase, 6-31G*). In THF **1c$_{oo}$·Mg-A** is 10.7 kcal/mol more stable than the separated reactants (6-31++G** values).

Starting from the most stable initial intermediate **1c$_{oo}$·Mg-A**, the kinetics of the first addition was investigated. Two transition states, one for the 1,2-addition (**1TS-1,2**) and the other one for the 1,4-addition (**1TS-1,4**), were located. Structures of both transition states are depicted in Figure 3, and their main geometrical parameters are collected in Table 2.

The kinetic preference for the 1,2-addition in the reaction of the first organomagnesium is clearly evinced by the calculations. While the 1,2-addition takes place with a low barrier (14.2 kcal/mol in THF), the 1,4-process exhibits a very high barrier (35.0 kcal/mol in THF). The reason for such high barrier is evident from the geometry of the 1,4-transition state. Transfer of the vinyl to the C-OR carbon, *trans* to the carbonyl interacting with the magnesium, entails a very strained structure. In order to keep the Mg···O=C interaction, during the vinyl transfer

(16) (a) Yamakazi, S.; Yamabe, S. *J. Org. Chem.* **2002**, *67*, 9346. (b) Ye, J. L.; Huang, P. Q.; Lu, X. *J. Org. Chem.* **2007**, *72*, 35, and references therein.

(17) (a) Holm, T.; Crossland, I. In *Grignard Reagents. New Developments*; Richey, H. G., Jr. Ed.; Wiley, Chichester, 2000; Chapter 1, pp 1. (b) Bickelhaupt, F. In *Grignard Reagents. New Developments*; Richey, H. G., Jr. Ed.; Wiley, Chichester, 2000; Chapter 9, p 299.

(18) (a) Tammiku-Taul, J.; Burk, P.; Tuulmets, A. J. *Phys. Chem.* **2004**, *108*, 133. (b) Mori, T.; Kato, S. *Chem. Phys. Lett.* **2007**, *437*, 159.

(19) Lefour, J. M.; Loupy, A. *Tetrahedron* **1977**, *34*, 2597.

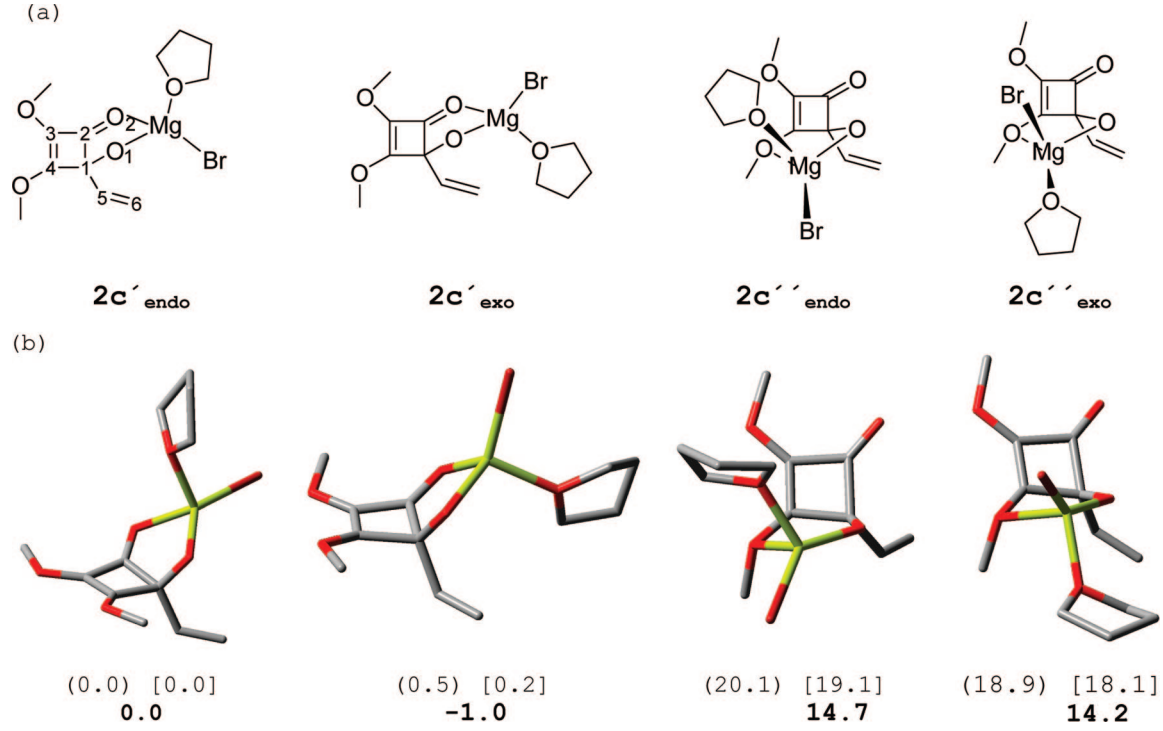

FIGURE 4. (a) Possible structures of alkoxide **2c** with four coordinated magnesium (carbon numbers C1−C4 are based on the starting squarate ring). (b) B3LYP/6-31G*-optimized geometries of alkoxides $\mathbf{2c'_{endo}}$, $\mathbf{2c'_{exo}}$, $\mathbf{2c''_{endo}}$, and $\mathbf{2c''_{exo}}$. The calculated energies ΔE (kcal/mol) are given in parentheses and $\Delta G_{(195K)}$ are given in brackets. The 6-31++G** energies in THF are in bold.

the squarate ring is severely distorted, the carbonyl group interacting with the magnesium being displaced above of the ring plane (**1TS-1,4**, Figure 3). As we will show later on this is not at all the case for the 1,4-addition of the second vinylmagnesium bromide. On the contrary, in the first 1,2-addition the vinyl is easily transferred to the carbon through a nonconstrained Mg···O=C···C four-membered cycle (**1TS-1,2**, Figure 3).

The first addition is a very exergonic process. Both the 1,2- and the 1,4-products are more than 30 kcal/mol more stable than the initial intermediate $\mathbf{1c_{oo}}$**·Mg-A**. In these products the magnesium is completing its tetracoordination by a bidentate coordination to two oxygens of the monoaddition product (Figure 3, Table 2). Interestingly, the 1,4-product is slightly more stable (about 2 kcal/mol) than the 1,2-addition product. This result points out a thermodynamic preference for the 1,4-addition, although for the first addition the huge difference in the energy barriers enforces a kinetic control of the reaction.

Product of the First 1,2-Addition. Optimization toward products starting from **1TS-1,2** leads to **1product-1,2**. This structure is one of the possible isomers of alkoxide **2c**, the product of the first 1,2-addition of vinylmagnesium bromide. We have explored several possible structures for such product. The four different possible structures considered are schematized in Figure 4. All of them have the four coordinated magnesium bonded to the alkoxide oxygen atom and the bromide anion. The third and fourth coordinating positions are occupied by a solvent molecule and either by the remaining carbonyl (**2c′**) or the methoxy group (**2c″**) as depicted in Figure 3. Two different structures result in each case when we consider the orientation of the coordinated THF: closer to the shorter or to the longer bridge of the bicyclic compound (exo and endo, respectively). Compounds type $\mathbf{2c'_{endo}}$ and $\mathbf{2c'_{exo}}$ with the magnesium coordinated to the carbonyl substituent were found to be much more stable than their isomers **2c″** (Figure 4). In THF the most stable species is $\mathbf{2c'_{exo}}$, with an structure equivalent to **1product-1,2**.

The preference for **2c′** structures can be ascribed to the higher partial δ^- borne by the carbonyl oxygen than by the methoxy oxygen. The polar resonance form of the carbonyl places a high negative NPA charge in the carbonyl oxygen of $\mathbf{2c'_{endo}}$ (−0.75). Conversely the negative charge on the methoxy oxygen interacting with the magnesium in $\mathbf{2c''_{endo}}$ is only −0.62. Given the large energy difference between complexes **2c′** and **2c″**, we disregard the latter as suitable reaction intermediates and continue with the former. $\mathbf{2c'_{endo}}$ and $\mathbf{2c'_{exo}}$ have very similar energies and can be exchanged by the dissociation of the THF molecule. Moreover similar intermediates can be obtained starting from either $\mathbf{2c'_{endo}}$ or $\mathbf{2c'_{exo}}$ by interaction with a second vinylmagnesium derivative.

The values of the coefficients of the p-orbitals in the LUMO and NPA charges for $\mathbf{2c'_{endo}}$ are given in Figure 5. The positive charge distribution is +0.46 e and +0.40 e at the carbonyl (C2) and the conjugate carbon (C4), respectively. The coefficients of the p-orbital of C2 and C4 in the LUMO have the same value, 0.56. On these grounds no remarkable selectivity in the reaction can be expected for electrostatic or orbital reasons. A previous coordination between the reactants to induce the observed selectivity is therefore suggested. Consequently, we have considered the coordination of the second vinylmagnesium bromide unity to **2c′** by interacting Mg(II) with the negatively charged alkoxy oxygen atom.

Addition of a Second Vinylmagnesium to the 1,2-Adduct 2: Competition between 1,2- and 1,4-Additions. With the aim of finding suitable intermediates for studying both the 1,2- and 1,4- pathways for the addition of the second organomagnesium, we have first investigated the possible isomers resulting from the complexation of $(CH_2CH)MgBr$·THF to **2c′**.

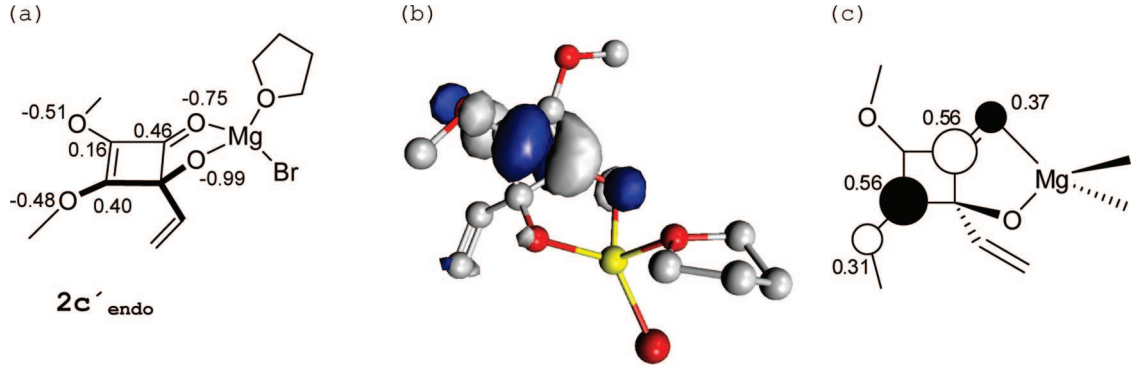

FIGURE 5. (a) NPA charges on selected atoms of $\mathbf{2c'}_{endo}$. (b) LUMO orbital. (c) Contribution of atomic p-orbitals in the LUMO.

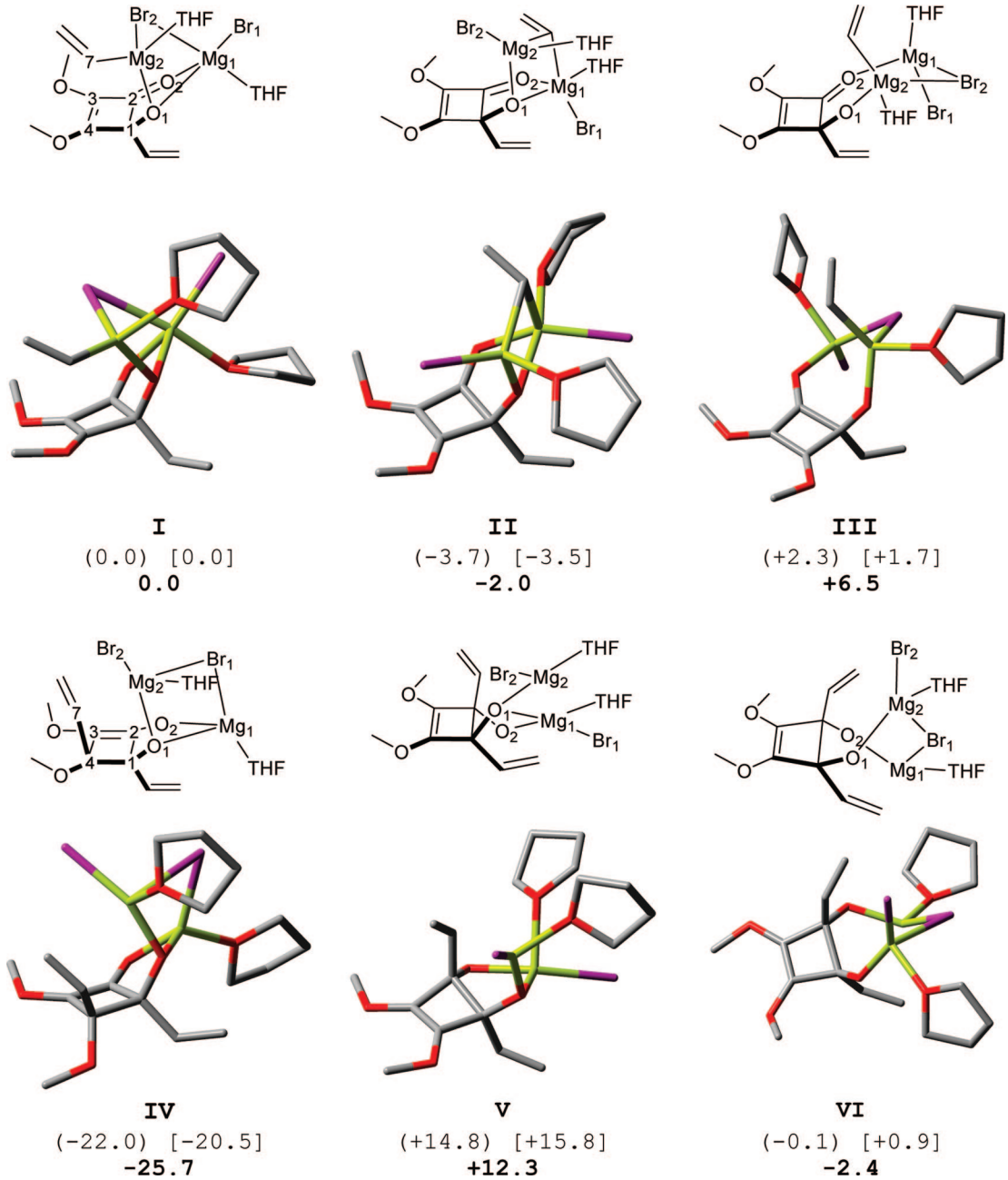

FIGURE 6. B3LYP/6-31G*-optimized geometries of intermediates **I**−**III** and addition products **IV**−**VI**. The calculated gas-phase potential energies (ΔE) and Gibbs energies ($\Delta G_{(195)}$) relative to **I** (in kcal/mol) are given in parentheses and in brackets, respectively. The 6-31++G** energies in THF are in bold.

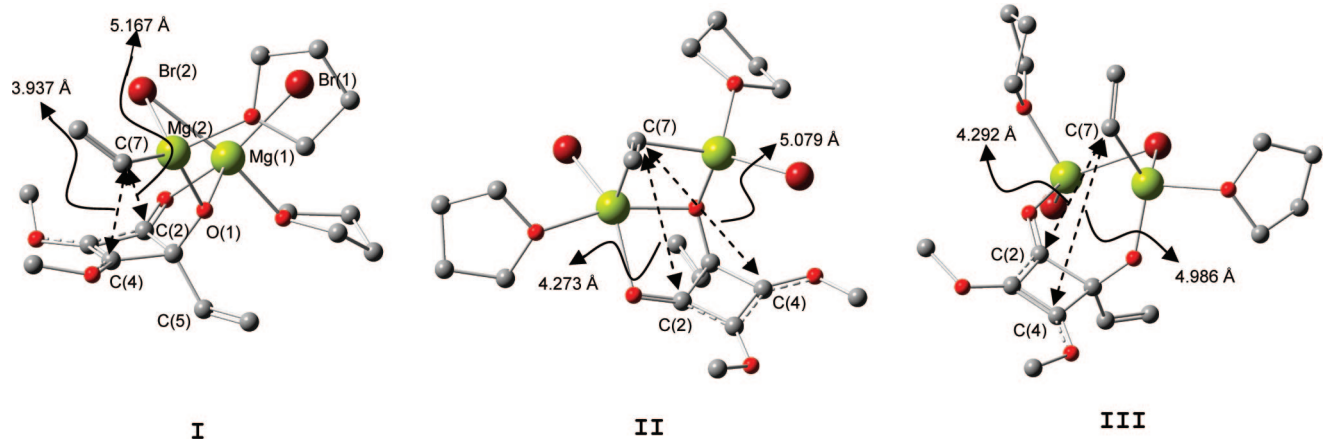

FIGURE 7. Optimized geometry of intermediates **I**−**III** showing the good orientation of the vinyl group for 1,4- (**I**) or 1,2-addition (**II** and **III**).

SCHEME 3. Possible Pathways to 1,2- and 1,4-Adducts from 2c′ through Complexation of $(CH_2CH)MgBr\cdot THF$[a]

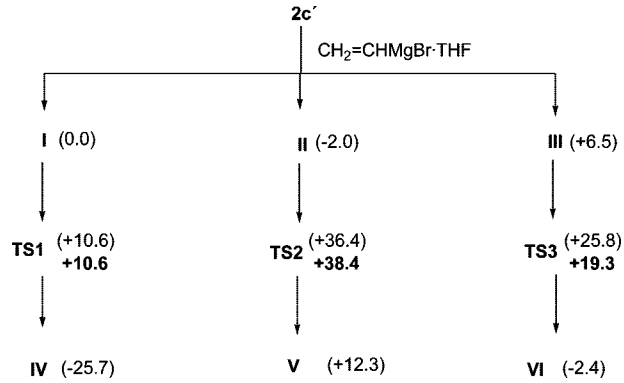

[a] The calculated B3LYP/6-31++G** energies in THF (kcal/mol) for intermediates and products relative to **I** and the energy barriers are given in parentheses and in bold, respectively.

The exploration of the possible isomers has resulted in three intermediates (**I**, **II**, and **III**) differing by less than 6 kcal/mol.

The optimized geometries and relative energies of intermediates **I**−**III** are shown in Figure 6. In structures **I** and **II** the magnesium atom of the first added organomagnesium keeps the same coordination than in **2c′**, quelating the oxygen atoms of the alkoxide and the carbonyl groups. The magnesium of the second organometallic reagent is coordinated to the alkoxy oxygen atom, with either its bromide (**I**) or vinyl (**II**) ligands bridging the first magnesium. Intermediate **III** presents a different coordination of the first magnesium atom, which is only coordinated to the carbonyl oxygen (distance Mg···Oalkoxy = 3.915 Å). This magnesium completes its four-coordination through a strong interaction with a bridging bromide coming from the second vinylmagnesium bromide. The energies of the three species are close: **II** is found 3.7 kcal/mol below **I**, whereas **III** lies 2.3 kcal/mol above **I** (gas-phase 6-31G* values). The relative Gibbs energies at 195 K are very similar to the relative energies, pointing out small entropic effects at this low temperature (Figure 6). Basis set extension and inclusion of solvent effects only slightly affects their relative energies: 6-31++G** values in THF are 0.0 (**I**), −2.0 (**II**), and +6.5 kcal/mol (**III**). The probable origin of the lower stability of **III** compared with that of **I** and **II** is the lower coordination number of the first magnesium in this structure. In **III** it is strictly tetracoordinated, whereas in **I** and **II** the magnesium atom has an additional interaction (4 + 1 coordination), with a bromide in **I** and with the π system of the vinyl in **II**. It could be expected that inclusion of more solvent molecules would level the energy of these structures. The complexation of the second organomagnesium derivative to **2c** is still more favored than the coordination of the first one to **1c**. In THF **I** is 26.8 kcal/mol more stable than separated $\mathbf{2c'_{exo}}$ and $(CH_2CH)MgBr\cdot THF$.

For geometric reasons, isomer **I** is a suitable intermediate to give the 1,4-addition. The vinyl moiety in **I** is oriented toward the electrophilic carbon C4, the vinyl carbon-C4 distance being 3.94 Å. In isomers **II** and **III** the vinyl carbon is placed above the C2 atom of the ring. On the same bases, isomers **II** and **III** can be considered as intermediates in the 1,2-addition (see Figure 7).

Scheme 3 shows the intermediates and reaction pathways studied for the second addition of the vinylmagnesium bromide through the complexation of $(CH_2CH)MgBr\cdot THF$ with alkoxide **2c′**.

Transition states for the transformation of intermediates **I**−**III** into the corresponding 1,2- or 1,4-adducts (**IV**−**VI**) were investigated. An initial exploration of the potential energy surface for the addition was performed taking as reaction coordinate the distance between the vinyl carbon C7 and the closest carbon atom of the ring (C2 or C4, depending on the intermediate). Then from the maximum of this monodimensional potential energy curve, the transition state was located and characterized in the full potential energy surface. Three TSs were found, one for the 1,4-addition (**TS1**) leading to the product **IV** and two for the 1,2-addition (**TS2** and **TS3**) leading to the **V** and **VI** products, respectively. Transition state structures are depicted in Figure 8. Selected structural data for intermediates, TSs,and addition products are given in Tables 3, 4, and 5. The atom numbering is shown in Figure 7.

In transition states **TS1** and **TS3** the transfer of the vinyl group from Mg2 to the carbon takes place with only minor changes in the coordination of the first magnesium (Mg1). In particular the bidentate coordination of Mg1 to both the O1 and O2 atoms is preserved in **TS1**, whereas in **TS3** it remains only coordinated to O2. The distances of the bonds being broken (Mg2−C7) and formed (C7−C4 or C7−C2) are very similar in both transition states. **TS2** involves a greater reorganization of the coordination of Mg1 because the vinyl being transferred was initially interacting with Mg1.

The 1,4-addition takes place with a low energy barrier of only 8.7 kcal/mol (6-31G* gas-phase value). Gibbs energy of

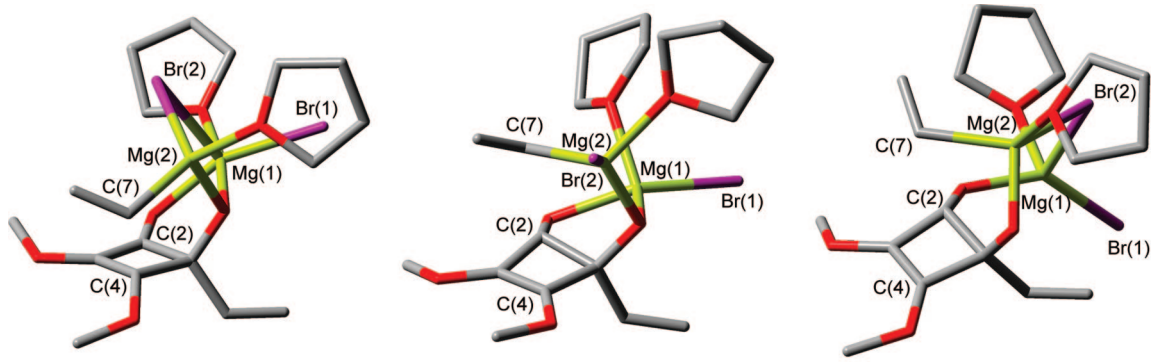

FIGURE 8. Optimized structures of **TS1**, **TS2**, and **TS3**. The calculated gas-phase potential energies (ΔE) and Gibbs energies ($\Delta G_{(195)}$) relative to **I** (in kcal/mol) are given in parentheses and in brackets, respectively. The 6-31++G** energies in THF are in bold.

TABLE 3. Selected Distances (Å) for Compounds in the Pathway I → IV

	I	TS1 (I → IV)	IV
d(Mg1−Br1)	2.463	2.471	2.488
d(Mg1−Br2)	2.734	2.739	4.544
d(Mg2−Br1	4.680	4.250	2.853
d(Mg2−Br2)	2.561	2.507	2.410
d(Mg2−C7)	2.109	2.167	2.887
d(C4−C7)	*3.938*	*2.181*	*1.508*
d(O1−Mg1)	2.091	2.117	2.035
d(O1−Mg2)	2.020	1.931	1.963
d(O2−Mg1)	2.140	2.082	1.960

TABLE 4. Selected Distances (Å) for Compounds in the Pathway II → V

	II	TS2 (II → V)	V
d(Mg1−Br1)	2.483	2.430	2.442
d(Mg1−C7)	2.323	3.119	3.082
d(Mg2−Br2)	2.433	2.409	2.391
d(Mg2−C7)	2.216	2.256	2.758
d(C2−C7)	*4.273*	*2.140*	*1.548*
d(O1−Mg1)	2.133	2.117	2.248
d(O1−Mg2)	1.974	1.953	1.906
d(O2−Mg1)	2.183	2.102	2.014

TABLE 5. Selected Distances (Å) for Compounds in the Pathway III → VI

	III	TS3 (III → VI)	VI
d(Mg1−Br1)	2.389	2.406	2.416
d(Mg1−Br2)	2.537	2.604	2.717
d(Mg2−Br2)	2.643	2.551	2.491
d(Mg2−C7)	2.123	2.174	2.531
d(C2−C7)	*4.292*	*2.199*	*1.512*
d(O1−Mg1)	3.915	4.172	4.251
d(O1−Mg2)	1.915	1.895	1.894
d(O2−Mg1)	2.001	1.957	1.903

activation at 195 K is almost the same (8.8 kcal/mol). Basis set extension and inclusion of solvent effects only slightly increase the barrier to 10.6 kcal/mol. Moreover the transformation of **I** into **IV** is a very exothermic process, the addition product **IV** lying 25.7 kcal/mol below **I** (6-31++G** in THF). Overall the 1,4-addition through the pathway **I → TS1 → IV** appears to be a very favorable process.

The two pathways explored for the 1,2-addition show very different energy barriers. In THF **TS2** is found 38.4 kcal/mol above the intermediate **II.** On the contrary the energy barrier in THF for reaching **TS3** from intermediate **III** is only 19.3 kcal/mol. Furthermore the addition product **VI** is considerably more stable than **V**. In the pathway **II → TS2 → V** the vinyl which is transferred from Mg2 to C2 is initially bridging Mg1, this interaction disappearing along the addition. Moreover the interaction between Mg1 and the alkoxy oxygen O1 is considerably decreased. Both factors redound in disfavoring this pathway. The pathway **III → TS3 → VI** is thus the most favored pathway for the 1,2-addition competing with the **I → TS1 → IV** transformation to deciding the regioselectivity of the addition. As found for intermediates, at 195 K entropic effects only slightly affect the energy barriers, just reducing the Gibbs energy difference between **TS1** and **TS3** by 0.8 kcal/mol. However increasing the temperature has an effect on the relative Gibbs energy of both transition states, **TS1** being mainly destabilized by entropic effects. At 298 K the Gibbs energies relative to **I** of **TS1** and **TS3** are 11.2 and 23.0 kcal/mol, respectively. Comparing with $\Delta G_{(195)}$ (Figure 8) the Gibbs energy difference between both TSs has been reduced from 15.1 to 11.8 kcal/mol. This result is in qualitative agreement with the observed significant decrease on regioselectivity when the temperature increases from −78 °C to room temperature (Table 1).

To assess the basis set influence on the 1,2- and 1,4-energy barriers, we have recalculated the energies in THF of intermediates **I** and **III** and transition states **TS1** and **TS3** with the triple-ζ 6-311++G** basis set. The main effect of this further basis set extension is stabilizing the species involved in the 1,2-addition: whereas **TS1** remains 10.6 kcal/mol above **I**, the relative energies of **III** and **TS3** are lowered from 6.5 and 25.8 kcal/mol (Scheme 3) to 1.2 and 20.2 kcal/mol, respectively. However energy barriers for the 1,4- and 1,2-additions are practically unaffected (6-311++G**, 10.6 and 19.0 kcal/mol; 6-31++G**, 10.6 and 19.3 kcal/mol) stressing the kinetic preference for the 1,4-pathway.

The difference between the calculated 6-31++G** energy barriers in THF of these two pathways (8.7 kcal/mol) would account for a complete regioselective 1,4-addition. The observed regioselectivity in the addition of 2 equiv of vinylmagnesium bromide in THF solution of **1c** is 92:8 in favor of the 1,4-addition product. Possibly a more extended model would be needed in the calculations to reproduce more accurately the experimental regioselectivity. Further calculations have been performed to discuss how the difference between the 1,4- and 1,2- barriers is influenced by the extension of the model.

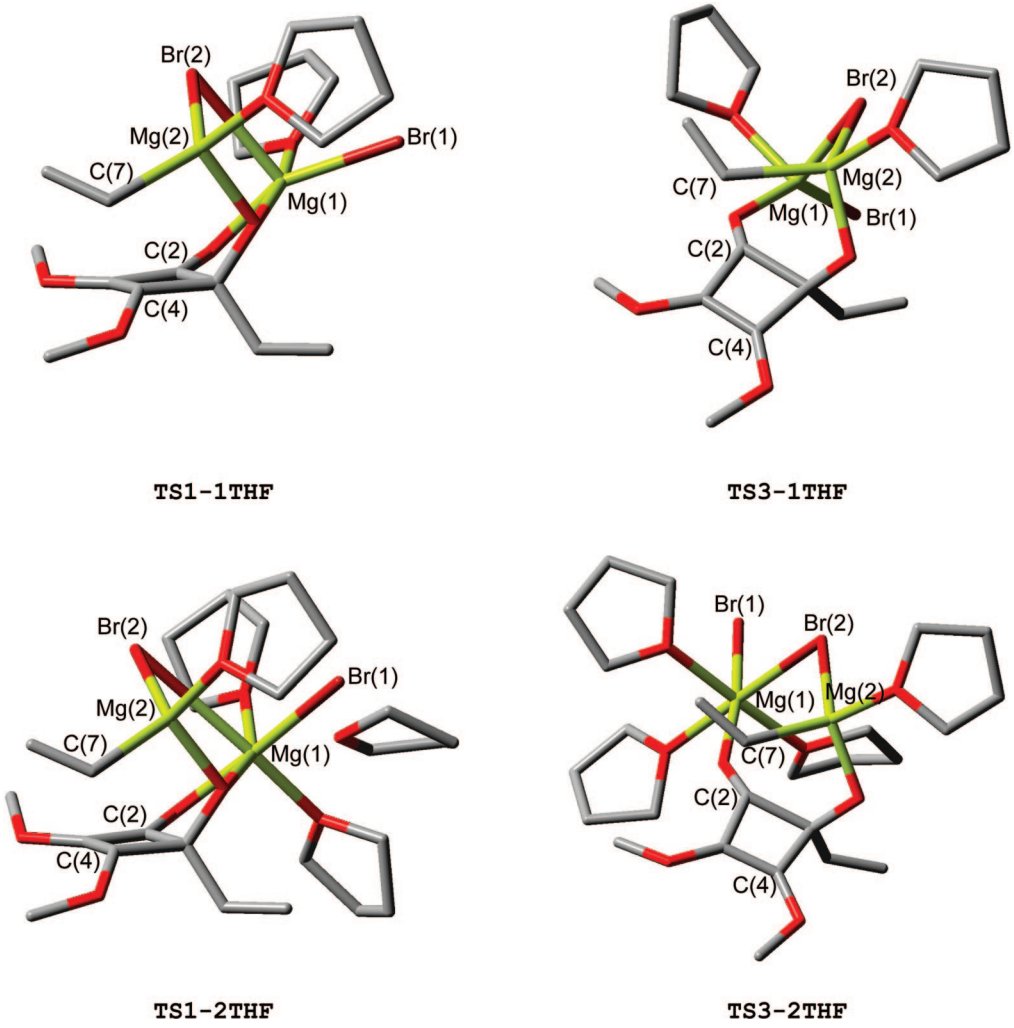

FIGURE 9. Optimized structures of **TS1−1THF**, **TS1−2THF**, **TS3−1THF**, and **TS3−2THF**.

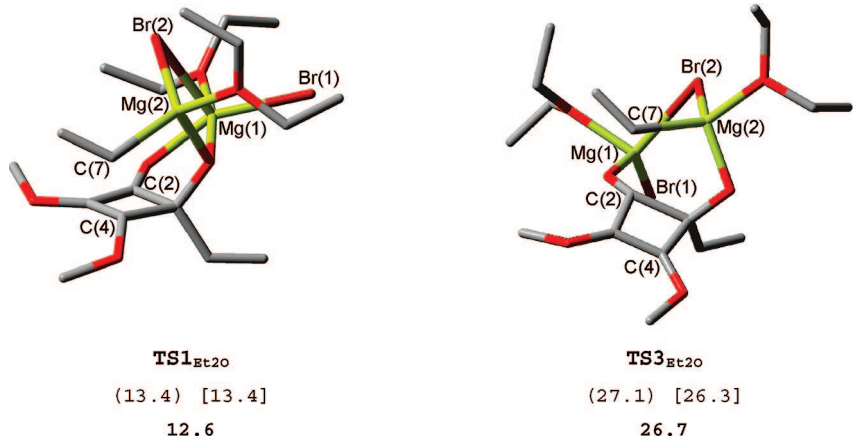

FIGURE 10. Optimized structures of $\mathbf{TS1}_{\mathbf{Et2O}}$ and $\mathbf{TS3}_{\mathbf{Et2O}}$. The calculated gas-phase potential energies (ΔE) and Gibbs energies ($\Delta G_{(195)}$) relative to $\mathbf{I}_{\mathbf{Et2O}}$ (in kcal/mol) are given in parentheses and in brackets, respectively. The 6-31++G** energies in diethyl ether are in bold.

The coordination of Mg2 is very similar in **TS1** and **TS3**, as they are the distances of the Mg−C and C−C breaking and forming bonds. The main differences are found in the coordination of Mg1. In **TS1** Mg1 is chelating oxygens 1 and 2 and coordinated to one THF molecule and two Br atoms, resulting in a square pyramidal 4 + 1 coordination. In **TS3** Mg1 is not coordinated to the alkoxy oxygen O1, giving an overall tetrahedral four-coordination. In order to estimate if the presence of additional solvent molecules could counterbalance this coordinative difference, we have reoptimized **TS1** and **TS3** with one and two additional THF molecules placed in the vicinity of Mg1. As the size of the system did not allow a full characterization of the transition states, we have kept fixed the Mg2−C7 and C7−C4 or C7−C2 distances at their values in **TS1** and **TS3**, the rest of the geometrical parameters being optimized.

The inclusion of one additional THF molecule has no effect on the energy difference between **TS1** and **TS3. TS1** was 15.2 kcal/mol more stable than **TS3** and **TS1−1THF** is 15.6 kcal/mol below **TS3−1THF** (6-31++G** energies in THF). Inspection of the geometries of **TS−1THF** and **TS3−1THF** gives the clues for this behavior. The additional THF molecule coordinates to Mg1 in both transition states, expanding the coordination of the Mg1 to octahedral in **TS1−1THF** and square pyramidal in **TS3-THF.** On the contrary, addition of a second THF molecule in the vicinity of Mg1 has an important effect, decreasing the energy difference between **TS1** and **TS3** to 7.2 kcal/mol (6-31++G** energies in THF).

The optimized structures of the transition states with one or two additional THF molecules (**TS1−1THF**, **TS3−1THF**, **TS1−2THF**, and **TS3−2THF**) are depicted in Figure 9. Whereas in **TS3−2THF** the second THF molecule retains its coordination to Mg1 after optimization, it remains out of the first coordination sphere of Mg1 in **TS1−2THF**, being placed far away from this magnesium atom (Mg1−O(THF) = 4.943 Å). The coordination number of Mg1 is the same in **TS1−2THF** and **TS3−2THF**, allowing for a more realistic comparison of their energies. However the 1,4-addition is still favored, pointing out the intrinsic preference for the 1,4-addition in this system. The possibility of retaining the quelation of Mg1 along the 1,4-addition pathway of the second organomagnesium reagent appears as a key feature governing the regioselectivity.

Influence of Solvent on 1,2- versus 1,4-Selectivity: Changing Diethyl Ether for THF. We have theoretically addressed the solvent effects on the regioselectivity of the addition of the second vinylmagnesium by studying the two most favorable pathways for the 1,4- and 1,2-additions (through **TS1** and **TS3**, respectively) using coordinated diethyl ether instead of THF and recalculating then the optimized structures in diethyl ether. Selected structural data for intermediates, TSs, and addition products are given in Supporting Information. Transition state structures $\mathbf{TS1}_{\mathbf{Et2O}}$ and $\mathbf{TS3}_{\mathbf{Et2O}}$ are depicted in Figure 10. Mg2−C7 and C7−C4/C7-C2 distances are very similar in transition states with diethyl ether and THF.

The energy barriers, including bulk solvent effects for both the 1,4- and 1,2-additions are slightly higher with ethyl ether than with THF (see Figure 11). $\mathbf{TS1}_{\mathbf{Et2O}}$ is found 12.6 kcal/mol above $\mathbf{I}_{\mathbf{Et2O}}$ (10.6 kcal/mol with THF) and $\mathbf{TS3}_{\mathbf{Et2O}}$ 19.4 kcal/mol above $\mathbf{III}_{\mathbf{Et2O}}$ (19.3 kcal/mol with THF). Indeed the difference between the energy barriers for the 1,4- and 1,2-addition is decreased from 8.7 kcal/mol in THF to 6.8 kcal/mol en diethyl ether. This computational result qualitatively agrees with the observed decreases of the regioselectivity when diethyl ether is substituted for THF (see entries 4 and 9, Table 1). Calculations trace out the destabilization of $\mathbf{TS1}_{\mathbf{Et2O}}$ with respect **TS1** as the main responsible for this decrease. As discussed for the THF complexes, an extended model including more diethyl ether molecules would be needed to account for the experimental regioselectivity (65:35 in favor of the 1,4-addition in **1a**, see Table 1).block

Summarizing, calculations are in agreement with the experimental results observed for the reaction of vinylmagnesium bromide with squarate **1c**, giving rise to the formation with a high regioselectivity of bicycloctenone **5c** by the 1,2/1,4 double addition. The intermediate **I**, resulting from the complexation between the 1,2-monoaddition alkoxide **2c** and the Grignard reagent, has been connected with the adduct **IV**, resulting from the 1,4-addition of the second vinyl group through **TS1**.

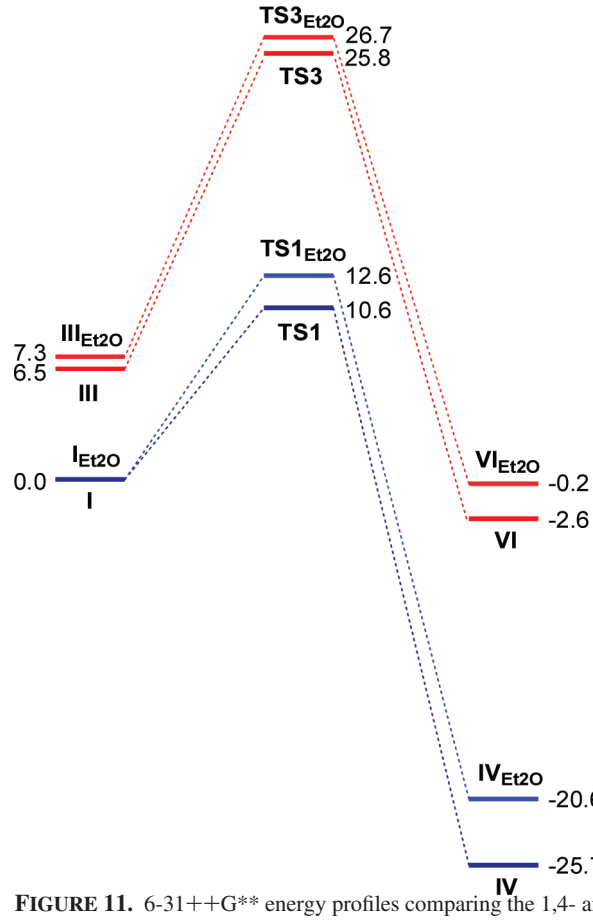

FIGURE 11. 6-31++G** energy profiles comparing the 1,4- and 1,2-additions in THF and diethyl ether (energies are in kcal/mol and relative to those of **I**).

Moreover, this pathway (**I** → **TS1** → **IV**), is seen to be the most favorable and involves the lower barrier and the most exothermic process (Figure 11). The alkoxide group in **2c** plays an essential role in the formation of intermediate **I**, in which the chelation of Mg1 seems to be the decisive factor to determine the regioselectivity observed.

Conclusions

The successive addition of 2 equiv of vinylmagnesium bromide to squarates constitutes an excellent framework to study the elements controlling the regio- and stereoselectivity of additions to substituted α,β-unsaturated ketones from the experimental as well as the theoretical point of view. The first Grignard equivalent adds to the carbonyl carbon exclusively, thus providing a γ-alkoxycyclobutenone. Calculations show a marked kinetic preference for the 1,2-addition in the first step, due to the very strained structure required for the transition state of the 1,4-addition. The process is very exergonic, with both the 1,2- and 1,4-products of the addition of the first organomagnesium having similar energies. Even the 1,4-product is slightly more stable, pointing out the possibility of addition through this pathway if the severe distortions in the transition state along this pathway could be relieved. Calculation of LUMO coefficients and NPA charges of the magnesium alkoxide does not allow expecting any regioselectivity in the addition of the second vinylmagnesium equivalent since LUMO coefficients and NPA charges in C-2 and C-4 show very similar values. Simplified models do not suggest any regioselectivity

in the addition of vinylmagnesium bromide to the α,β-unsaturated moiety since alkoxide-coordinated Mg(II) is placed at a similar distance to both electrophilic centers. However, according to the experimental data this addition takes place with very remarkable regioselectivity giving rise to the formation of the 1,4- and the 1,2-addition products in a 9:1 ratio. B3LYP/6-31++G** calculations including solvent effects show the existence of a lower energy transition state leading to the 1,4-addition product from an intermediate involving the coordination of the second vinylmagnesium bromide unity by interacting tetracoordinated Mg(II) with the negatively charged alkoxy oxygen atom. Energetically less favorable TSs lead to the formation of 1,2-addition products and account for the experimental regioselectivity. Consequently, our study clearly demonstrates that the regioselectivity attained in the conjugate addition is controlled by complex induced proximity effects (CIPE). Comparison of the energy profiles for the first and the second organomagnesium 1,2- and 1,4- additions shows that CIPE affects both the kinetics and the termodynamics of the vinylmagnesium addition, lowering the barrier for the 1,4- compared to the 1,2-addition and increasing the stability of the 1,4-product.

Experimental Section

3,4-Dibutoxy-4-hydroxy-4-vinylcyclobut-2-enone (3a). A solution of the Grignard reagent (2 mmol) in 20 mL of anhydrous THF was slowly added under inert atmosphere (N_2 or Ar) to a solution of diketone **1a** (226 mg, 1 mmol) in anhydrous THF (20 mL) at −78 °C. The mixture was stirred for 2 h at this temperature and then hydrolyzed with saturated aqueous NH_4Cl (10 mL). After the bath was removed and the mixture reached room temperature, 10 mL of water was added. The aqueous layer was then separated, and the organic layer was extracted with EtOAc (3 × 15 mL). The combined organic layers were dried with Na_2SO_4, and the solvent was eliminated to give 250 mg of a crude mixture where the alcohol **3a** was the only main product (NMR). Purification by column chromatography (silica gel, hexanes/ethyl acetate, 6:1) yielded 135 mg (0.53 mmol, 53% yield) of **3a** as an oil. ^{1}H NMR (300 MHz $CDCl_3$): δ (ppm) 5.97 (dd, J = 17.3 and 10.7 Hz, 1H), 5.50 (dd, J = 17.3 and 0.9 Hz, 1H), 5.32 (dd, J = 10.7 and 0.9 Hz, 1H), 4.27−4.45 (m, 2H), 4.22 (t, J = 6.5 Hz, 2H), 1.51−1.75 (m, 4H), 1.25− 1.48 (m, 4H), 0.95 (m, 6H). ^{13}C NMR (75.4 MHz, $CDCl_3$): δ (ppm) 185.0 (C), 166.7 (C), 134.7 (CH), 133.1 (C), 118.0 (CH_2), 86.5 (C), 72.9 (CH_2), 70.6 (CH_2), 31.6 (CH_2), 31.3 (CH_2), 18.6 (CH_2), 18.5 (CH_2), 13.6 (CH_3), 13.5 (CH_3). IR (thin film): 3375, 2955, 2869, 1766, 1695, 1616, 1464, 1410 cm^{-1}. HRMS (CI) m/z (MH^+) calcd for $C_{14}H_{23}O_4$ 255.1599, found 255.1598.

General Procedure for the Formation of Bicyclic α-Hydroxyketones 5. Addition of Vinylmagnesium Bromide to Squarates 1 (Procedure A).[20] A solution of the squarate **1** (1 mmol) in THF (10 mL) was slowly added under N_2 at −78 °C to a stirred solution of the vinylmagnesium bromide (6 mmol) in anhydrous THF (15 mL). The reaction mixture was allowed to reach slowly room temperature in the dry ice−acetone bath. Both stirring and the N_2 flow were maintained for another 4 h at room temperature before quenching with a saturated sodium bicarbonate solution. After 30 min, the organic layer was separated, and the aqueous layer was extracted three times with ethyl acetate. The combined organic extracts were washed with brine, dried over Na_2SO_4, and filtered. After concentration, the resulting residue was analyzed by NMR and/or GC before purification by flash chromatography. Yields for each experiment are reported in Table 1.[21]

(20) Addition of a six-fold excess of organometallic reagents was necessary in order to avoid contamination of the products due to the presence of monoaddition adducts.

General Procedure for the Formation of Bicyclic γ-Hydroxyketones 7. Addition of Vinyllithium to Squarates 1 (Procedure B). A total of 3.8 mL of MeLi 1.6 M (6 mmol) in anhydrous THF (5 mL) was slowly added under N_2 at 0 °C to a stirred solution of tetravinyltin[22] (1.5 mmol) in anhydrous THF (10 mL). Stirring was maintained at this temperature for 30 min before the ice bath was removed. After reaching room temperature and always under a positive N_2 flow, the reaction mixture was cooled at −78 °C. Then, a solution of the squarate **1** (1 mmol) in anhydrous THF (10 mL) was slowly added. From this point onward the procedure follows that described for the addition of vinylmagnesium bromide (Procedure A). Yields for each experiment are reported in Table 1.[21]

(3a*R,6a*R**)-2,3-Dibutoxy-6a-hydroxy-4,5,6,6a-tetrahydropentalen-1(3a*H*)-one (5a).** Following the general Procedure A, 168 mg (0.59 mmol) of bicyclotenone **5a** was obtained as an oil from **1a** (1 mmol) after purification by column chromatography (deactivated silica gel, hexanes/ethyl acetate, 9:1) (59% yield). ^{1}H NMR (300 MHz, $CDCl_3$): δ (ppm) 4.28−4.50 (m, 2H), 3.96 (t, J= 6.6 Hz, 2H), 2.78 (d, J = 7.3 Hz, 1H), 1.48−1.98 (m, 8H), 1.22−1.42 (m, 6H), 0.89 (t, J = 7.3 Hz, 3H), 0.86 (t, J = 7.3 Hz, 3H). ^{13}C NMR (75.4 MHz, $CDCl_3$): δ (ppm) 201.3 (C), 171.5 (C), 132.77 (C), 82.5 (C), 71.3 (CH_2), 71.1 (CH_2), 49.1 (CH), 37.0 (CH_2), 31.8 (CH_2), 31.5 (CH_2), 27.2 (CH_2), 24.0 (CH_2), 18.8 (CH_2), 18.6 (CH_2), 13.6 (CH_3), 13.5 (CH_3). IR (thin film): 3396, 2956, 2869, 1700, 1607, 1463, 1407 cm^{-1}. HRMS (EI) m/z (M^+) calcd for $C_{16}H_{26}O_4$ 282.1831, found 282.1829.

(3a*R,6a*R**)-6a-Hydroxy-2,3-diisopropoxy-4,5,6,6a-tetrahydropentalen-1(3a*H*)-one (5b).** In an Ar atmosphere, following the general Procedure A, 68 mg (0.26 mmol) of bicyclotenone **5b** was obtained as an oil from **1b** (1 mmol) after purification by column chromatography (deactivated silica gel, hexanes/ethyl acetate, 9:1) (26% yield). ^{1}H NMR (300 MHz, $CDCl_3$): δ (ppm) 5.30 (sept, J = 6.0 Hz, 1H), 4.85 (sept, J = 6.0 Hz, 1H), 3.20 (bs, 1 OH), 2.80 (d, J = 8.3 Hz, 1H), 1.95 (m, 1H), 1.60−1.90 (m, 5H), 1.32(d, J = 6.0 Hz, 3H), 1.26 (d, J = 6.0 Hz, 3H), 1.21 (d, J = 6.0 Hz, 3H), 1.18 (d, J = 6.0 Hz, 3H). ^{13}C NMR (75.4 MHz, $CDCl_3$): δ (ppm) 201.3 (C), 171.0 (C), 131.1(C), 82.5 (C), 73.9 (CH), 71.7 (CH), 49.4 (CH), 37.4 (CH_2), 27.4 (CH_2), 24.0 (CH_2), 22.7 (CH_3), 22.6 (CH_3), 22.4 (CH_3), 22.4 (CH_3). IR (thin film): 3408, 2974, 2934, 2872, 1699, 1601, 1466, 1308, 1099 cm^{-1}. HRMS (EI) m/z: (M^+) calcd for $C_{14}H_{22}O_4$ 254.1518, found 254.1506.

(3a*R,6a*R**)-6a-Hydroxy-2,3-dimethoxy-4,5,6,6a-tetrahydropentalen-1(3a*H*)-one (5c).** Following the general Procedure A, 120 mg (0.6 mmol) of bicyclotenone **5c** was obtained as an oil from **1c** (1 mmol) after purification by column chromatography (deactivated silica gel, hexanes/ethyl acetate, 4:1) (60% yield). ^{1}H NMR (300 MHz, $CDCl_3$): δ (ppm) 4.05 (s, 3H), 3.74 (s, 3H), 2.80 (d, J = 7.9 Hz, 1H), 1.55−1.95 (m, 5H), 1.30− 1.45 (m, 1H). ^{13}C NMR (75.4 MHz, $CDCl_3$): δ (ppm) 201.1 (C), 172.0 (C), 133.9 (C), 82.7 (C), 59.5 (CH_3), 59.0 (CH_3), 48.7 (CH), 37.0 (CH_2), 27.2 (CH_2), 24.1 (CH_2). IR (thin film): 3406, 2958, 2870, 1699, 1614, 1462, 1343, 1099 cm^{-1}. HRMS (EI) m/z: (M^+) calcd for $C_{10}H_{14}O_4$ 198.0892, found 198.0893.

(3a*R,6a*R**)-2,3-Dibutoxy-3a-hydroxy-4,5,6,6a-tetrahydropentalen-1(3a*H*)-one (7a).** Following the general Procedure B, 161 mg (0.57 mmol) of bicyclotenone **7a** was obtained as an oil from **1a** (1 mmol) after purification by column chromatography (deactivated silica gel, hexanes/ethyl acetate, 9:1) (57% yield). ^{1}H NMR (300 MHz, $CDCl_3$): δ (ppm) 4.37−4.46 (m, 2H), 3.92−4.05 (m, 2H), 2.45 (dd, J = 8.2 Hz, J = 3.2 Hz, 1H), 2.05−2.20 (m, 1H),

(21) Reaction crude was constituted by bicyclic hydroxyketones **5** and/or **7** only contaminated by minor impurities (see Supporting Information). Purification by column chromatography with commercial or deactivated (triethylamine) silica or alumina did not allow us to obtain better values for the yield of isolated products. The purification method was not optimized. The values reported in the table correspond to those obtained with triethylamine treated silica.

(22) Nugent, W. A.; Hobbs, F. W. *J. Org. Chem.* **1986**, *51*, 3376.

1.85−1.95 (m, 7H), 1.32−1.55 (m, 6H), 0.89 (t, J = 7.3 Hz, 3H), 0.86 (t, J = 7.3 Hz, 3H). ^{13}C NMR (75.4 MHz, $CDCl_3$): δ (ppm) 200.2 (C), 167.7 (C), 134.5 (C), 82.1 (C), 71.5 (CH_2), 71.47 (CH_2), 55.1 (CH), 36.9 (CH_2), 31.9 (CH_2), 31.6 (CH_2), 27.6 (CH_2), 24.7 (CH_2), 18.9 (CH_2), 18.7 (CH_2), 13.7 (CH_3), 13.6 (CH_3). IR (thin film): 3393, 2956, 2868, 1698, 1615, 1463, 1406 cm^{-1}. HRMS (EI) m/z (M^+) calcd for $C_{16}H_{26}O_4$ 282.1831, found 282.1833.

(3a*R,6a*R**)-3a-Hydroxy-2,3-diisopropoxy-4,5,6,6a-tetrahydropentalen-1(3a*H*)-one (7b).**[10c] Following the general Procedure B in Ar atmosphere, 118 mg (0.46 mmol) of bicycloctenone **7b** was obtained as an oil from **1b** (1 mmol) after purification by column chromatography (deactivated silica gel, hexanes/ethyl acetate, 9:1) (46% yield). ^{1}H NMR (300 MHz, $CDCl_3$): δ (ppm) 5.35 (sept, J = 6.0 Hz, 1H), 4.89 (sept, J = 6.0 Hz, 1H), 2.70 (bs, 1 OH), 2.5 (dd, J = 9.4 Hz, J = 2.6 Hz, 1H), 2.07 (m, 1H), 1.50−1.90 (m, 5H), 1.3 (d, J = 6.0 Hz, 3H), 1.21 (d, J = 6.0 Hz, 3H), 1.18 (d, J = 6.0 Hz, 3H), 1.12 (d, J = 6.0 Hz, 3H). ^{13}C NMR (75.4 MHz, $CDCl_3$): δ (ppm) 200.3 (C), 167.5 (C), 132.5 (C), 82.1 (C), 73.7 (CH), 71.8 (CH), 55.8 (CH), 37.0 (CH_2), 27.7 (CH_2), 24.7 (CH_2), 22.6 (CH_3), 22.46 (2 × CH_3), 22.42 (CH_3). IR (thin film): 3403, 2978, 2934, 2874, 1691, 1612, 1381, 1308, 1101 cm^{-1}. HRMS (EI) m/z (M^+) calcd for $C_{14}H_{22}O_4$ 254.1518, found 254.1514.

(3a*R,6a*R**)-3a-Hydroxy-2,3-dimethoxy-4,5,6,6a-tetrahydropentalen-1(3a*H*)-one (7c).** Following the general Procedure B, 88 mg of bicycloctenone **7c** (0.44 mmol) was obtained as an oil from **1c** (1 mmol) after purification by column chromatography (deactivated silica gel, hexanes/ethyl acetate, 4:1) (44% yield). ^{1}H NMR (300 MHz, $CDCl_3$): δ (ppm) 4.13 (s, 3H), 3.75 (s, 3H), 2.70 (bs, 1 OH), 2.5 (d, J = 7.0 Hz, 1H), 2.09 (dd, J = 12.0 and 6.0 Hz, 1H), 1.60−1.85 (m, 4H), 1.20− 1.38 (m, 1H). ^{13}C NMR (75.4 MHz, $CDCl_3$): δ (ppm) 200.1 (C), 168.4 (C), 135.6 (C), 82.1 (C), 59.7 (CH_3), 59.4 (CH_3), 55.4 (CH), 36.9 (CH_2), 27.6 (CH_2), 24.9 (CH_2). IR (thin film): 3383, 2956, 2869, 1698, 1633, 1462, 1335 cm^{-1}. HRMS (EI) m/z (M^+) calcd for $C_{10}H_{14}O_4$ 198.0892, found 198.0884.

2,3-Dibutoxy-4-methoxy-4-vinylcyclobut-2-enone (8a). Following the method described in the literature,[15] 0.53 mg of pure **8a** (1.98 mmol) was obtained from 2.4 mmol of **3a** (82%). ^{1}H NMR (300 MHz, $CDCl_3$): δ (ppm) 5.85 (dd, J = 17.0 and 10.5 Hz, 1H), 5.43 (dd, J = 17 and 1.1 Hz, 1H), 5.26 (dd, J = 10.5 and 1.1 Hz), 4.28 (t, J = 7 Jz, 2H), 4.20 (t, J = 7 Hz, 2H), 3.30 (s, 3H), 1.75−1.55 (m, 4H), 1.35 (m, 4H), 0.88 (t, J = 7 Hz, 3H), 0.87 (t, J = 7 Hz, 3H). ^{13}C NMR (75.4 MHz, $CDCl_3$): δ (ppm) 184.1 (C), 165.6 (C), 134.4 (CH), 133.7 (C), 118.2 (CH_2), 92.0 (C), 72.9 (CH_2), 70.7 (CH_2), 52.2 (CH_3), 31.7 (CH_2), 31.4 (CH_2), 18.6 (CH_2), 18.5 (CH_2), 13.6 (CH_3), 13.5 (CH_3). IR (thin film): 2955, 2869, 1766, 1695, 1616, 1464, 1410 cm^{-1}. HRMS (EI) m/z (M^+) calcd for $C_{15}H_{24}O_4$ 268.1675, found 268.1680.

2,3-Dibutoxy-4-trimethylsilyloxy-4-vinylcyclobut-2-enone (9a). A solution of trimethylsilyl triflate (0.320 mL, 1.77 mmol) in 10 mL of diethyl ether was slowly added in N_2 atmosphere to a solution of the alcohol **3a** (300 mg, 1.18 mmol) and 0.5 mL of Et_3N in anhydrous diethyl ether (20 mL) at 0 °C. After stirring for 20 min, the reaction mixture was quenched with 10 mL of a 2% $NaHCO_3$ aqueous solution. Usual workup afforded 377 mg (1.15 mmol, 98% yield) of pure **9a** as an oil, which was identified by NMR and HRMS. ^{1}H NMR (300 MHz, $CDCl_3$): δ (ppm) 5.87 (dd, J = 17.2 and 10.5 Hz, 1H), 5.37 (dd, J = 17.2 and 1.1 Hz, 1H), 5.20 (dd, J = 10.5 and 1.1 Hz), 4.30 (m, 2H), 4.18 (t, J = 6.5 Hz, 2H) 1.70-1.50 (m, 4H), 1.36 (m, 4H), 0.89 (t, J = 6.5 Hz, 3H), 0.87 (t, J = 6.5 Hz, 3H), 0.1 (s, 9H). ^{13}C NMR (75.4 MHz, $CDCl_3$): δ (ppm) 184.5 (C), 166.9 (C), 135.9 (CH), 133.2 (C), 117.2 (CH_2), 88.1 (C), 72.7 (CH_2), 70.5 (CH_2), 31.7 (CH_2), 31.3 (CH_2), 18.6 (CH_2), 18.5 (CH_2), 13.5 (CH_3), 13.4 (CH_3), 1.0 (3xCH_3). IR (thin film): 2960, 2875, 1776, 1641, 1330, 1252 cm^{-1}. HRMS (EI) m/z (M+) calcd for $C_{17}H_{30}O_4Si$ 326.1913, found 326.1906.

Computational Details. All calculations were carried out with the Gaussian 03 program package[23] using the B3LYP[24,25] density functional. The structures of the reactants, intermediates, transition states and products were fully optimized in the gas phase without any symmetry restrictions using the 6-31G* basis set for all atoms.[26–28] Frequency calculations were performed on all the 6-31G* optimized structures to characterize the stationary points as minima or transition states, as well as for the calculation of Gibbs energies at 195 K ($\Delta G_{(195)}$). The connection between transition states and their corresponding reactants and products was checked by fully optimizing structures derived from the transition states with a small displacement following the transition vector in both directions. Bulk solvent effects were taken into account with the CPCM polarized continuum model[29] (THF, ϵ = 7.58; diethyl ether, ϵ = 4.335) by means of single-point 6-31++G** calculations at the 6-31G* gas-phase optimized geometries.[26–28,30] To check up the basis set influence on the 1,2- and 1,4- energy barriers the energies in THF of selected species were recalculated with and extended triple-ζ 6-311++G** basis set.

Acknowledgment. Financial support by the Spanish Dirección General de Investigación Científica y Técnica (BQU2003-00315/CTQ2006-28333-E, CTQ2005-09000-C02-01 and Project Consolider Ingenio 2010 CSD2007-00006) is gratefully acknowledged. A.A. thanks the Spanish Ministerio de Educación for a fellowship. We gratefully acknowledge SCSIE (Universidad de Valencia) for access to the instrumental facilities.

Supporting Information Available: General experimental information; representative ^{13}C NMR spectrum and gas chromatogram of the crude reaction mixture obtained for a typical experiment between **1a** and vinylmagnesium bromide in THF at −78 °C (entry 4, Table 1); copies of ^{1}H and ^{13}C NMR spectra of compounds **3a**, **5a−c**, **7a−c**, **8a** and **9a**; B3LYP/6-31G* optimized structures, Cartesian coordinates and gas phase and CPCM energies of all optimized structures; selected structural data for intermediates, TSs and addition products with coordinated diethyl ether. This material is available free of charge via the Internet at http://pubs.acs.org.

JO800617Y

(23) Frisch, M. J.; Trucks, G. W.; Schlegel, H. B.; Scuseria, G. E.; Robb, M. A.; Cheeseman, J. R.; Montgomery, J. A.; Vreven, T. J.; Kudin, K. N. ; Burant, J. C.; Millan, J. M. ; Iyegar, S. S.; Tomasi, J.; Barone, V.; Mennucci, B.; Cossi, M.; Scalmani, G.; Rega, N.; Petersson, G. A.; Nakatsuji, H.; Hada, M.; Ehara, M.; Toyota, K.; Fukuda, R.; Hasegawa, J.; Ishida, M.; Nakajima, T.; Honda, Y. ; Kitao, O.; Nakai, H.; Klene, M.; Li, X.; Knox, J. E.; Hratchian, H. P.; Cross, J. B.; Adamo, C.; Jaramillo, J.; Gomperts, R.; Stratmann, R. E.; Yazyev, O.; Austin, A. J.; Cammi, R.; Pomelli, C.; Ochterski, J. W.; Ayala, P. Y.; Morokuma, K.; Voth, G. A.; Salvador, P.; Dannenberg, J. J.; Zakrzewski, V. G.; Dapprich, S.; Daniels, A. D.; Strain, M. C.; Farkas, O.; Malick, D. K.; Rabuck, A. D.; Raghavachari, K.; Foresman, J. B.; Ortiz, J. V.; Cui, Q.; Baboul, A. G.; Clifford, S.; Cioslowski, J.; Stefanov, B. B.; Liu, G.; Liashenko, A.; Clifford, S.; Komaroni, I.; Martin, R. L.; Fox, D. J.; Keith, T.; Al-Laham, M. A.; Peng, C. Y.; Nanayakkara, A.; Challacombe, M.; Gill, P. M. W.; Johnson, B.; Chen, W.; Wong, M. W.; Gonzalez, C.; Pople, J. A. *Gaussian 03, Revision C.02*; Gaussian, Inc.: Wallingford, CT, 2004.

(24) Becke, A. D. *J. Chem. Phys.* **1993**, *98*, 5648.

(25) Lee, C.; Yang, W.; Parr, R. G. *Phys. Rev. B: Condens. Matter Mater. Phys.* **1988**, *37*, 785.

(26) Hehre, W. J.; Ditchfield, R.; Pople, J. A. *J. Phys. Chem.* **1972**, *56*, 2257.

(27) Hariharan, P. C.; Pople, J. A. *Theor. Chim. Acta.* **1973**, *28*, 213.

(28) Francl, M. M.; Pietro, W. J.; Hehre, W. J.; Binkley, J. S.; Gordon, M. S.; DeFrees, D. J.; Pople, J. A. *J. Chem. Phys.* **1982**, *77*, 3654.

(29) Barone, V.; Cossi, M. *J. Phys. Chem. A* **1998**, *102*, 1995.

(30) Rassolov, V. A.; Pople, J. A.; Ratner, M. A.; Windus, T. L. *J. Chem. Phys.* **1998**, *109*, 1223.